Effect of light impurities on the electronic structure of copper nanowires

E. P. M. Amorim[1,2] and E. Z. da Silva[1]

[1]*Institute of Physics "Gleb Wataghin," University of Campinas–Unicamp, 13083-970 Campinas, SP, Brazil*

[2]*Departamento de Física, Universidade do Estado de Santa Catarina, 89219-710 Joinville, SC, Brazil*

(Received 19 May 2011; revised manuscript received 17 January 2012; published 4 April 2012)

Recently an interesting mechanochemical effect was found showing a possibility to produce longer copper atomic chains in nitrogen atmospheres [Amorim and da Silva, Phys. Rev. B **82**, 153403 (2010)]. This work presents a systematic and comparative study of the effect of doping with H, B, C, N, O, S, and N_2 impurities to the electronic structure of copper nanowires. It was performed by means of *ab initio* total energy calculations based on density functional theory, using local density and generalized gradient approximations. All impurities show a sd_{z^2} bond, boron makes a σpd_{yz} bond, while carbon, oxygen, and sulfur have a strong σpd_{z^2} and πpd_{yz} bond. These impurities modify the metallic chain structure of the nanowire and change chain distances in the way that can be observed in electron microscopy experiments. Nitrogen and N_2 also have a strong σpd_{z^2} and make a πpd_{xz} bond that is stronger than the other impurities enhancing the size of atomic chains. Small spin anisotropy is introduced through carbon, oxygen, nitrogen, and sulfur doping. Remarks about the electronic states around the Fermi level are presented.

DOI: 10.1103/PhysRevB.85.155407 PACS number(s): 61.46.−w, 62.25.−g, 71.15.Pd, 73.22.−f

I. INTRODUCTION

The problem of producing nanoconductors has been intensely studied in the last two decades. From the experimental point of view, the evolution from bulk to nanowires (NWs) and ultimately to one-atom-thick metal NWs or linear atomic chains (LACs) was observed in many different experiments. High-resolution transmission electron microscopy (HRTEM) images, as well as the quantized conductance plateaus measured for long periods of time using a mechanically controlled break junction (MCBJ) or scanning tunneling microscopy (STM) all have showed consolidated evidence of their stability and the ability to manipulate these new structures.[1]

There are interesting basic science studies that reported interesting possibilities for technological applications to *recreate* electronics at the nanoscale. For example, fullerene inserted into gold breaking junctions has a current per voltage transistor profile,[2] and copper atomic chains deposited on Cu (111)[3–5] and gold atomic chains deposited in NiAl (110)[6] showed one-dimensional band behavior for larger distances due to a decoupling between surface and atomic chain electronic states. There are also new proposals to change the electronic paradigm, such as spintronic. In that way, cobalt impurities in copper and gold atomic chains as prototype systems for spin filters present exciting possibilities.[7,8]

Besides the magnetic impurities mentioned above, the study of some light impurities was very fruitful to predict new phenomena and to support experimental interpretations. For example, the large LAC bonds in thin gold NWs observed in HRTEM images[9] were attributed to impurities not observed in such experiments. Sparked by these results, many theoretical works using *ab initio* techniques[10–14] were devoted to calculate the most probable candidates to explain these abnormal distances. In this process novel effects were predicted, sometimes providing inspiration to the experimentalists. A successful example is the oxygen impurity enhancing the atomic chain in gold NWs, increasing their LAC lengths, that was theoretically predicted[15] and experimentally verified.[16]

Although gold was the first metal intensively studied as a candidate for nanocontacts, copper has also attracted a lot of attention. Our recent work studying copper NWs through tight-binding molecular dynamics (TBMD) simulations showed the formation of short LACs[17] and using *ab initio* calculations also discussed details of their electronic structure.[18] Noncrystalline structures such as multishell, helical, or tubular shapes have been studied for many metals[19–22] and observed by means of HRTEM images for gold[23,24] and platinum.[25] Many theoretical works have investigated these structural possibilities in copper NWs as well.[26–30]

Nanomaterials have their mechanical properties strongly related to their chemical bonds. Their ability of changing coordination numbers and bond properties, as they evolve to one-dimensional structures, is referenced as a mechanochemical effect. The increase of gold LAC lengths induced by impurities[15,16] or by a particular axial stress[21,22] presents examples of this kind of effect. However, this effect is not restricted to gold. The mechanochemical relation between thiolates and gold which allow one to pull a string of gold atoms from a gold surface[31] was also investigated in the case of copper,[32,33] as well as the incorporation of N and N_2 into copper LACs that enhance their strength, causing the rearrangement of their tips and producing larger LACs.[34]

A detailed investigation of the interaction of atomic and molecular light impurities with nanocontacts and nanowires is essential for both fundamental and applied perspectives; therefore in this work we study this very important problem, that has been addressed in the case of gold nanowires, with very interesting results and consequences:[10–13,15,16] how bonds are formed between copper and light impurities in these extremely low-coordination Cu LACs. This is a very interesting question because in short LACs, one impurity causes a great deal of change in the electronic properties of the system, and these effects can be observed in the enhancement of bond lengths by HRTEM experiments. For this purpose, we performed *ab initio* total energy calculations based on density functional theory for realistic copper NWs, doped with H, B, C, N, O,

S, and N_2 impurities. The NWs used in the present study are realistic since they were obtained from the molecular dynamics evolution of stretched NWs that evolved to the formation of linear atomic chains of coper atoms attached to realistic tips,[17] similar to experiments. The next section presents technical calculation details. Section III discusses the electronic structure of the doped NWs showing the projected density of states per orbital for each case, presenting remarks about the electronic states at the Fermi level. Details of the local density of states and total charge of density help to clarify all bond types and the anisotropy introduced by each impurity. All calculations were performed for two exchange-correlation approximations, and major differences between them are presented.

II. CALCULATION DETAILS

The *ab initio* total energy studies based on density functional theory (DFT)[35,36] were used in self-consistent calculations to search for the minimum electronic density and, therefore, find the total energy of the ground state of copper NWs doped with light impurities. The SIESTA method was employed to perform the calculations.[37] The interaction between copper valence states ($3d^{10}$ $4s^1$) and core electrons was described by norm-conserving Troullier-Martins pseudopotentials[38] with nonlocal partial-core corrections.[39] The local density[40] and generalized gradient[41] approximations (LDA and GGA) were used to obtain the exchange-correlation (XC) energy. Split valence double-zeta basis (spin polarized) and localized numerical orbitals with a confining energy of 0.08 and 0.18 eV for LDA and GGA, respectively, were chosen to represent the electronic wave-function basis sets. The charge density grid was defined with a cutoff energies of 200 Ry for LDA and 300 Ry for GGA to perform the relaxation from the insertion of impurity until the NW break. This grid was increased to 400 Ry for both XC approximations in order to calculate the density of states and charges of all systems considered. Reference 18 shows calculations performed for copper bulk and dimers to check the quality of these parameters and the pseudopotential used.

The original structure was obtained from a copper bulk truncated along the [111] crystallographic direction forming a stack of three layers with seven, six, and seven atoms repeated four times (80 atoms). Previous work studied this structure, that was relaxed using tight-binding molecular dynamics by an annealing procedure to a cylindrical shape NW which was stretched several times evolving to a LAC formation and consequently to its rupture.[17] From the annealed configuration before the rupture, we started an *ab initio* calculation relaxing the structure by a conjugated gradient (CG) where the stretching of the copper NW was achieved by pulling it quasistatically until its rupture.[18] The present study uses this LDA relaxed NW configuration before the rupture, which was exposed to each impurity. The procedure consists of the following four steps: (1) one impurity was placed close to the first LAC bond, (2) the whole NW structure was elongated along the stretching axis by 0.1 Å, (3) a CG calculation was performed until all force components were smaller than 0.01 eV/Å, and (4) steps 2–3 were repeated until the observation of tip retraction or a sudden increase of one LAC bond indicating the NW rupture. This evolution was performed first using LDA, and to save computational efforts, the GGA calculation was done from the LDA NW before rupture, evolving similarly through the CG procedure described above, until the rupture. This NW was defined enclosed in a supercell with dimensions $(30, 30, 38 < L < 46)$ Å where L is the NW length and the Brillouin zone sampling was represented by 8 k points along its axis.[42]

III. ELECTRONIC STRUCTURE

In the study of thin metal NWs, interesting questions became important. Long bond distances in gold NWs sparkled interest in the effect of impurities in these low coordinated structures. In the case of copper, HRTEM images show metallic NWs stretched along [100], [110], and [111] crystallographic directions evolving to LACs in all cases. The LAC is a low coordination structure under tension, attached by higher coordination tips. Copper, in particular, evolved to smaller atomic chains than gold NWs. Our calculations have demonstrated that LAC lengths could vary from two to four atoms performed with tight-binding molecular dynamics calculations for the different orientations[17] or up to three atoms from *ab initio* results.[18] From these results, we chose the [111] structure to perform the present study, doping it with light impurities. Therefore, we allow the [111] structure to relax with each impurity close to its first LAC bond (from left to right) by means of conjugated gradient procedure, minimizing the forces to search for a local energy minimum in a quasistatic way. These relaxations revealed a general trend in which all impurities formed strong bonds with the metal atoms remaining stable bridging copper atoms, and favoring the NW break at a pure Cu-Cu bond. Among these impurities, N and N_2 stood out as peculiar cases because their bonds with LAC atoms are so stable and strong that they could be used to pull atoms from the tips, enhancing the atomic chain and revealing an interesting mechanochemical effect.[34]

From the configuration before the rupture, the calculated electronic structure was used to understand the nature of bonds between copper and impurities in this extreme situation, far from copper in bulk. In Figs. 1 to 7, we present the density of valence states projected per orbital (PDOS) for copper and all impurities (H, B, C, N, O, S, and N_2, respectively). These figures follow the same presentation: The top panel shows the [111] copper NW with each impurity showing the atomic distances and the breaking bond (red/gray arrow), the middle panels show, respectively, copper d and s states, and the bottom ones show the impurity valence states. All calculations were performed using LDA and GGA exchange-correlation approximations, but the figures show only the GGA results, and the major differences between these approximations are discussed in the text. The insets enclosed in these panels show the local density of states (LDOS) plotted around narrow energies from one up to four peaks through the isolines (black for spin up and red/gray for spin down) varying from 0.0001 electrons/bohr^3 to 0.1 electrons/bohr^3 together with a 0.001 electrons/bohr^3 isosurface (yellow/light gray) allowing identification of different bond possibilities between copper and each impurity. The range of energies are indicated in each figure caption (from Figs. 1 to 7), and the peaks are referenced

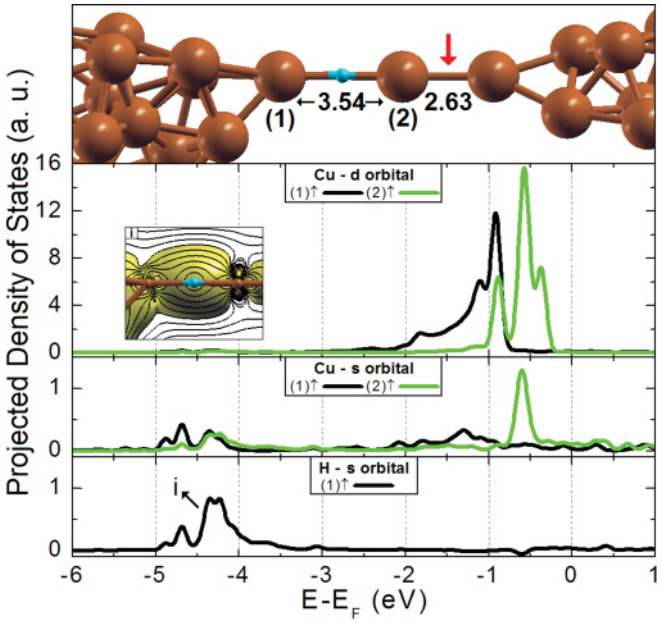

FIG. 1. (Color online) Projected density of states (PDOS) of copper NW with H evidencing the local DOS of peak i, (-3.75 ± 1.25) eV.

from left to right, considering just occupied states up to the Fermi level.

Figure 1 shows the density of states projected per orbital for some Cu LAC atoms and the hydrogen impurity. The states calculated with GGA are closer to the Fermi level and more localized than the LDA ones for atom 1, while for atom 2 the states are just localized without shifting to the Fermi level in the GGA approach compared to LDA. Peak i shows a sd_{z^2} bond type with a high delocalization of the s electron of hydrogen, but evidently bonded to a d_{z^2} state from atom 2. As the orbital d_{z^2} is the most localized with a favorable spatial overlap with the copper s orbital, we could see also a contribution from this orbital in peak i.

Figure 2 displays the PDOS of the Cu LAC with B impurity with two kinds of bonds: (1) sd_{z^2} as in the hydrogen case above and other (2) σpd_{yz}. In this case, the s orbital is more localized about -6.7 eV, probably due to the closed shell s state with two electrons in opposition to the hydrogen case above, which is more delocalized, as we can see comparing the isosurface between this sd_{z^2} bond with the previous case above. Although both isosurfaces are similar, the volume occupied in the boron case is smaller, indicating a stronger localization and density than the hydrogen case. If we compare these two bond isosurfaces, the charge density is larger for peak i than for peak ii, which is what we can conclude observing the difference in peak intensity between the two bonds, with peak i being a much more localized state than ii, which can be explained since the p state has one electron in an open shell state.

Figure 3 shows the PDOS of the Cu LAC with C impurity. First, this case presents a slim spin anisotropy given by the energy difference between up and down states. In this case, there are three kinds of bonds: peak i shows clearly a sd_{z^2} similar to the cases discussed above, peak ii exhibits a σpd_{z^2}, while peak iii is a πpd_{yz} the weakest bond as seen through the isosurface which occupies a bigger volume than peak ii. From Hund's rule, if we have one p electron, mandatorily, a second p electron should have the same spin, remaining spatially far

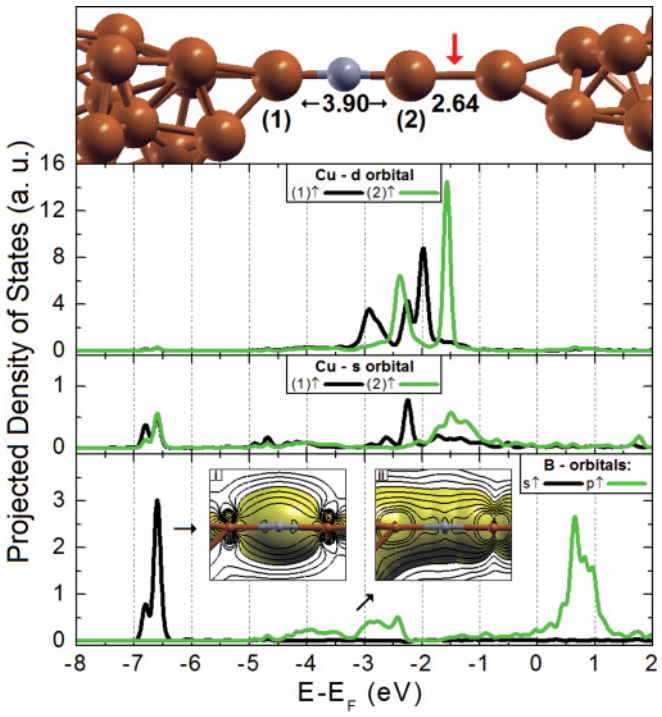

FIG. 2. (Color online) Projected density of states (PDOS) of copper NW with B, showing peaks i, (-6.67 ± 0.34) eV, and ii, (-3.59 ± 1.41) eV, in the local DOS insets.

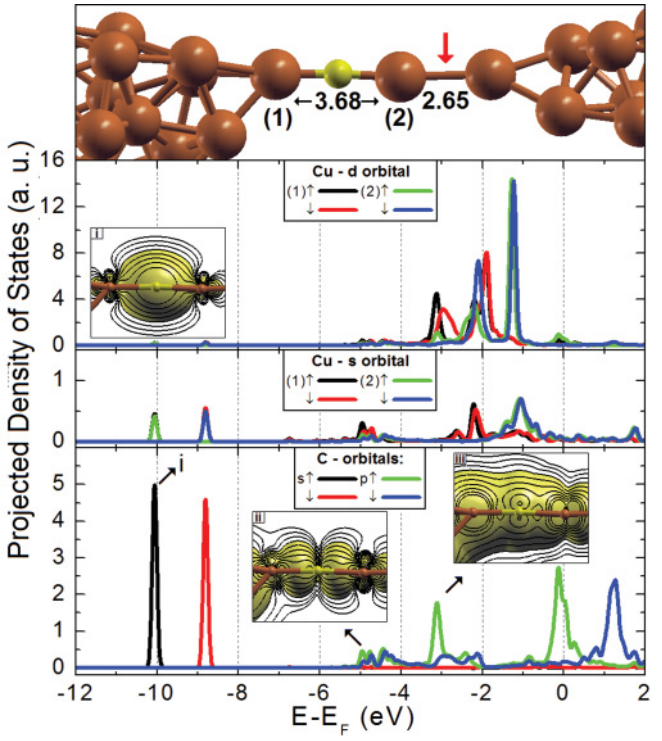

FIG. 3. (Color online) Projected density of states (PDOS) of copper NW with C; LDOS insets show peaks i, (-10.05 ± 0.20) eV; ii, (-4.58 ± 0.83) eV; and iii, (-2.80 ± 0.95) eV.

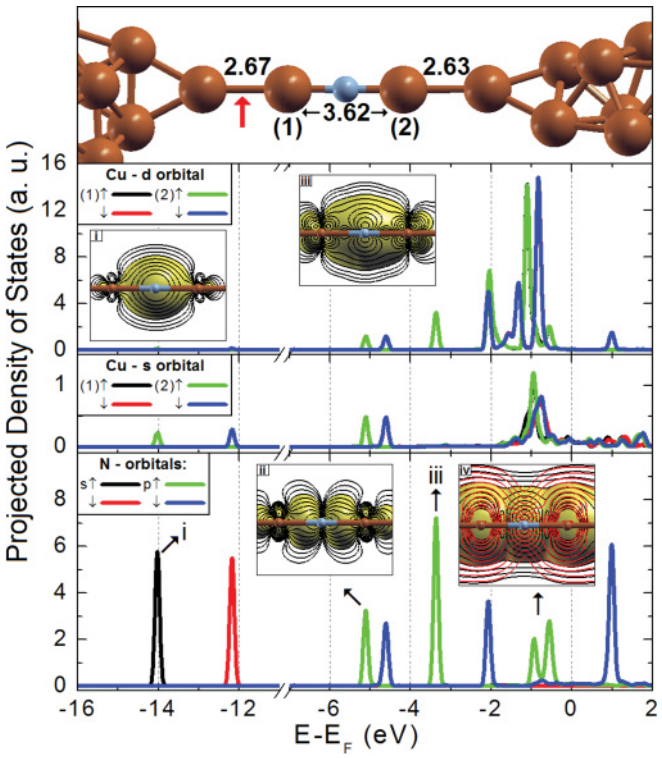

FIG. 4. (Color online) Projected density of states (PDOS) of copper NW with N, LDOS insets show the peaks: i, (-14.05 ± 0.20) eV; ii, (-5.10 ± 0.20) eV; iii, (-3.35 ± 0.20) eV; and iv, (-0.71 ± 0.45) eV. The first three insets are spin up (black), and the last one is spin up and down superposed (black and red). From Ref. 34 with modifications.

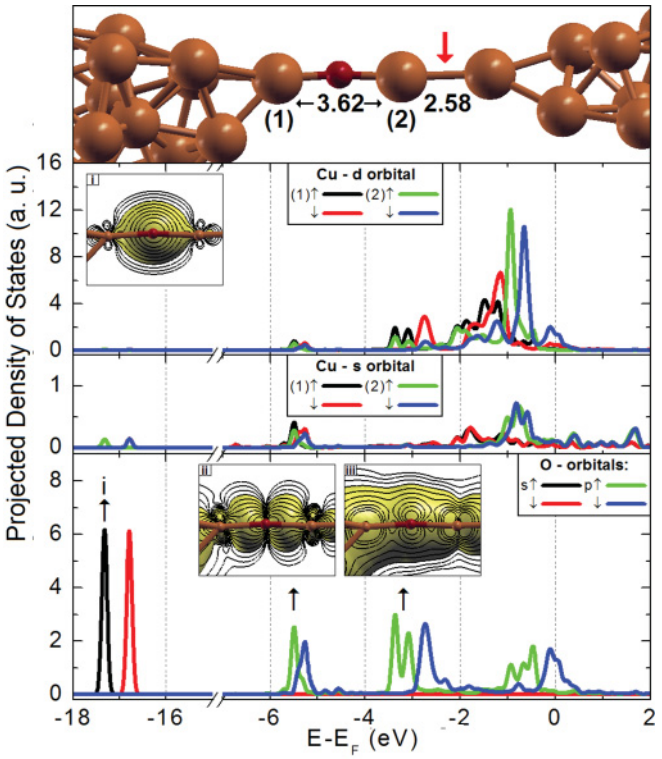

FIG. 5. (Color online) Projected density of states (PDOS) of copper NW with O, showing the LDOS insets with these peaks: i, (-17.33 ± 0.20) eV; ii, (-5.13 ± 0.73) eV; and iii, (-2.63 ± 1.09) eV.

from the first one; due to the Pauli principle it does not occupy the same p state. This becomes clear when we observe two distinct situations for each p electron in peaks ii and iii; they are perpendicular orbitals.

Figure 4 displays the PDOS for the Cu LAC with N. In this distinct case, we observe the mechanochemical effect which causes the reconstruction of tips, enhancing the atomic chain size, resulting in a longer LAC,[34] clearly evidencing the strong bond formed between copper and nitrogen in this low coordination situation. This case shows two s electrons in peak i and three p electrons respectively for peaks ii, iii, and iv. Peak i shows a sd_{z^2} bond with a contribution of s orbital from copper as explained before. The first two peaks associated to the p electrons evidence a (ii) σpd_{z^2} and (iii) πpd_{xz}. In this case, differently from the previous cases, we can see two strong bonds in which both isosurfaces are much smaller than we observed up till now. In other words, two perpendicular electronic p states make bonds with two distinct kinds of d orbitals. The last peak (iv) reveals a strong anisotropy close to the Fermi level forming a weak bond (largest isosurface) compared with the others with a π bond for spin up (black lines) and a σ one for spin down (red lines).

Therefore, we observe in a natural way the electron occupancy of the p states. On the one hand, from the lower energy states up to the Fermi level, in the carbon case (Fig. 3), the first p electron in peak ii makes a strong bond, while the other p electron in peak iii makes a weak bond. On the other hand, the nitrogen has more localized p states around their energies, and the first p electron as well the second one make significantly strong bonds, clearly showed by their smaller isosurfaces. The last electron near the Fermi level has a weak bond related to a considerable spin anisotropy. In a distinct way, the three p electrons make perpendicular orbital bonds, observing a combination of two kinds of bonds between p and d states, characterized by a high charge density in peaks ii and iii which enhances the bonding between copper and nitrogen and allows tip reconstruction; therefore it aids the increment of Cu atoms extracted from the tips, which are incorporated into the LAC when the NW is stretched.

Figure 5 displays the PDOS of the Cu LAC doped with O. This case shows a spin anisotropy as in the carbon case, which is not associated to a p state in special as the nitrogen case. This could be understood in the follow way: Carbon has two spin up p electrons kept spatially far enough having a small anisotropy, while oxygen has four p electrons, three of them with spin up and one with spin down. Therefore, the oxygen has two p electrons in the same state and again, two p electrons with spin up, spatially far, producing as in the carbon case a small anisotropy. In the case of nitrogen with three p electrons in different p states, there is a considerable anisotropy due to the correlation of these three electrons, introducing at the same time the strong localization around well-defined energies. The oxygen case has more localized states than hydrogen, boron, and carbon, but, however, not so much as nitrogen. Peak i is associated to a sd_{z^2} bond as found in the other impurities,

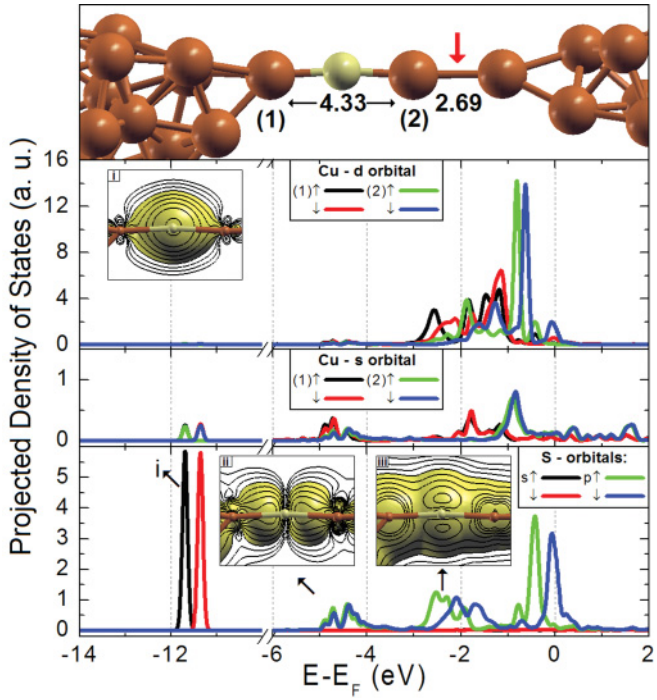

FIG. 6. (Color online) Projected density of states (PDOS) of copper NW with S, detaching the peaks in the LDOS insets: i, (-11.53 ± 0.38) eV; ii, (-4.15 ± 0.90) eV; and iii, (-2.13 ± 1.13) eV.

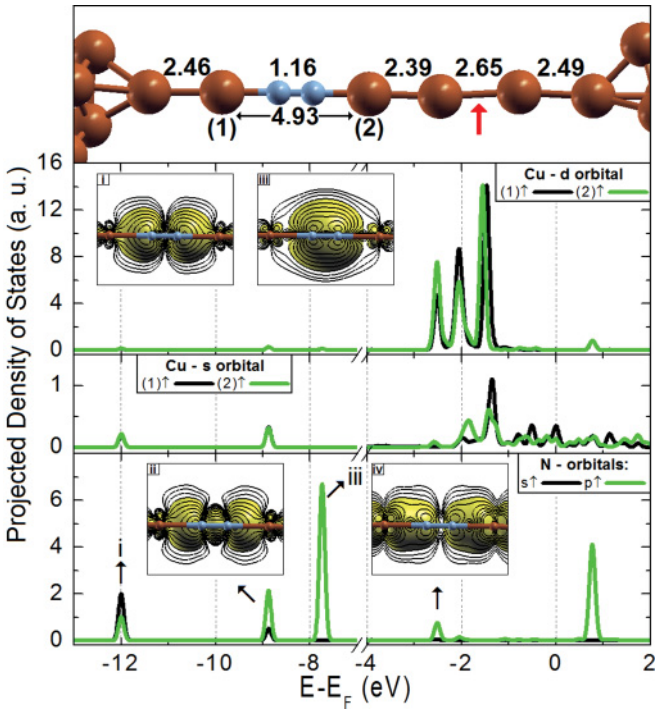

FIG. 7. (Color online) Projected density of states (PDOS) of copper NW with N_2 with the following peaks in the LDOS insets: i, (-12.00 ± 0.20) eV, (-8.88 ± 0.20) eV, (-7.75 ± 0.21) eV, e (-2.50 ± 0.20) eV. From Ref. 34 with modifications.

peak ii to a σpd_{z^2} state, clearly the strongest between the other p states, while peak iii is a πpd_{yz} similar to the carbon case.

Figure 6 shows the PDOS of Cu LAC with S. This case is is very similar to the oxygen, since they are isoelectronic. Peak i presents a sd_{z^2} character, peak ii a σpd_{z^2}, and peak iii is a πpd_{yz} similar to the cases of carbon and oxygen. Sulfur as well as carbon and oxygen have a very similar electronic structure, due to the electronic distribution of the p states, as explained above. S is the impurity that makes the largest impact in the Cu-X-Cu bond (where X stands for the impurity), similar to the effect of a small diatomic molecule.

The general trend due to the insertion of a light impurity is the development of a large fictitious Cu-Cu bond that is in fact a Cu-X-Cu bond. While Cu-Cu bonds tend to be in the range of around 2.2 to 2.7 Å, the large distances provided by the effect of the atomic impurities are 3.47/3.54 Å for H, 3.91/3.90 Å for B, 3.66/3.68 Å for C, 3.62/3.62 Å for N, 3.60/3.62 Å for O, and the largest of all 4.32/4.33 Å for S, respectively, for LDA/GGA XC calculations.[34] These results correlate well with the order of the covalent radii of these elements, and HRTEM images similar to the ones produced in the case of Au NWs could verify these values.

Figure 7 displays the PDOS of the LAC doped with N_2 impurity where we observed also the mechanochemical effect attributed to the incorporation of nitrogen.[34] This last case shows a contribution from copper s and p orbitals indicating an hybridization between these orbitals with an sd_{z^2} bond, observed in all other cases, and a spd_z^2 bond for peak i, with strong influence of charge isolines from the s orbital. Peak ii shows again a spd_z^2 hybridization, the strongest one, but in this case with the charge isolines between nitrogen atoms display a σ bond between p orbitals from each nitrogen, clearly the stronger and at the lower dimer bond energy. Peak iii exhibits a π dimer bond, but even so this bond is weaker than the σ bond; it has the highest density and has been the most probable. In peak iv we observe again a strong πpd_{xz} bond as in the nitrogen case, but in the N_2 case, we can see a high concentration of charge, evidencing the possibility that the doping of N_2 could make the bond stronger than the single N case, what we indeed found because the LAC with N_2 evolved under tension to six copper atoms, the longer LAC obtained through the doping of one a single impurity.[34] Differences regarding the spin states were not observed.

In the H, B, C, O, and S cases (Figs. 1–3, 5, and 6) we can see that the DOS from atom 2, the right neighbor of the impurity, is more shifted toward the Fermi level than atom 1, the left neighbor of the impurity. This happened due to the difference in coordination between these two atoms;[18] in other words, atom 2 is two coordinated, while atom 1 is three coordinated, bonded to the impurity and to two Cu atoms from the tip. The case of N and N_2 are different, due to the mechanochemical effect; in these cases a LAC reconstruction turned both neighbor atoms around the impurity into two-coordinated Cu atoms with similar bond distances, due to this effect, and the DOS from atoms 1 and 2 are essentially the same as can be seen in Figs. 4 and 7.

From these results, the analysis of electronic states occupation could be done in the following way: first, when one electron occupies a s or p state, its DOS is much more delocalized, as observed for hydrogen and boron, both have delocalized s and p orbitals, respectively. The increase of occupation by another p electron forms a σpd_{z^2} bond as the

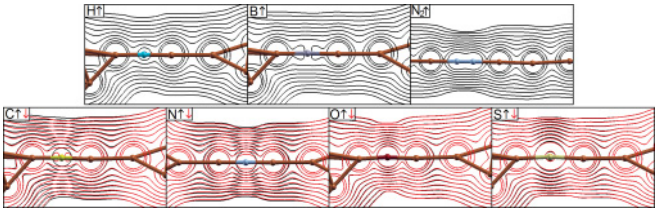

FIG. 8. (Color online) Total charge density from 0.0001 electrons/bohr^3 to 0.1 electrons/bohr^3 (logarithmic scale) for LAC with each impurity. The top panel shows the H, B, and N_2, and the bottom panel shows C, N, O, and S where lines black and red (gray) are, respectively, spin up and down.

lowest energy p state, followed by a π pd_{xz} for the N and N_2 cases and π pd_{yz} for the other cases. Therefore, as we expected, there is a tendency for the σ bond to appear at lower energies than π bonds, as we observed in all cases.

In general, all results show LDOS of both spin peaks without significant differences concerning the local charge density when the states are integrated until the Fermi level. The only exception is peak iv in the N case as showed. However, if we consider the total charge density, these differences could be seen more clearly.

Figure 8 displays the total charge density integrated up to the Fermi level for all cases. The top and bottom panel show the cases without and with spin anisotropy. For the cases without spin anisotropy, the charge isoline configurations are very similar for H and N_2 with a spherical shape around the impurity, although the charge concentration around the N_2 is much larger, evidencing the strong bond between Cu and N, beyond the bigger charge concentration. The isolines joining the impurities and their copper neighbors are respectively the eighth for H and B and ninth for N_2, corresponding respectively to 0.013 and 0.036 electrons/bohr^3. In the case of B, the p predominant orbital is associated to the charge density shape, differently from the H and N_2 cases, which are associated with s orbitals. Considering the cases with spin anisotropy (bottom panel), C and N cases have a visible anisotropy, while both O and S do not have considerable differences comparing their isolines between spin up and down. All cases with anisotropy have charge densities with spherical symmetry. Regarding the LDA and GGA approximations, just the O impurity shows a larger charge concentration in the GGA than in LDA. In all cases the eighth line (0.013 electrons/bohr^3) joins the impurities to their copper neighbors.

The knowledge of the LDOS below Fermi level is interesting to help us determine the nature of the bonds formed. However, the existence of occupied electronic states at the Fermi level is a mandatory condition to observe ballistic conduction across the LAC with a light impurity. There are peaks associated to C, O, and S impurities with a large portion above the Fermi level, representing unoccupied states. The analysis of isosurfaces and the distribution of electronic states showed an absence of bonds between copper and these impurities around the Fermi level, what actually we expected to find. The other impurities, namely, H, B, N, and N_2, all have shy PDOS values around the Fermi level. Table I shows a summary of all bonds formed between copper with all impurities showing in a large picture the main differences regarding all bonds and an analysis of the electronic states at the Fermi level. This analysis compares the percentage of DOS from s and p states, respectively, for spins up (↑) and down (↓). The H, B, and N_2 cases show the same values for both spins, revealing the absence of spin anisotropy as we showed above in Fig. 5. The impurities with p states have a smaller s-state percentage compared to the p ones where the C case has the lower s percentage around 0.3% and and N_2 has a s state corresponding to half of the p state (16%) at the Fermi level. The spin anisotropy is more pronounced for the s state of N and for the p state of C, O, and S. The O and S cases are especially interesting. There is no spin anisotropy when these impurities were incorporated to the NWs, the situation in which the angle between the LAC and impurity is smaller than 180°. This result indicates that the spin anisotropy was induced by tension to form the linear configuration of the LAC in these cases. On the other hand, N shows a smaller spin anisotropy in the linear configuration as compared to the initial configuration (about 30% and 70% for p↑ and p↓ states) as well as a smaller contribution from the s state per spin (<0.01%).

IV. CONCLUSIONS

In this work *ab initio* calculations were used to study the effect of light impurities to the electronic properties of doped realistic copper NWs, from their insertion into the LAC and their evolution, up to the NW rupture, observing their bond distances to the copper atoms. Our work shows what kind of bond these impurities make and the effect they have on the structural properties of these NWs. The knowledge of these bond distances should be useful to compare with HRTEM images, enlightening the question about which impurity is doping the NW. Among the impurities studied, N and N_2 stood

TABLE I. Summary of bonds between copper atoms from LAC and all impurities and energy percentage per spins up and down for s and p states at Fermi level (LDA and GGA).

Electronic structure	s	p	s bond	p bond	LDA (s↑, s↓, p↑, p↓) (%)	GGA (s↑, s↓, p↑, p↓) (%)
H 1s^1	↑				50.00, 50.00	50.11, 49.89
B [He] 2s^2 2p^1	↑↓	↑,		σ d$_{yz}$	2.12, 2.12, 47.88, 47.88	1.67, 1.67, 48.33, 48.33
C [He] 2s^2 2p^2	↑↓	↑, ↑,	σ d$_{z^2}$	σ d$_{z^2}$, π d$_{yz}$	0.26, 0.33, 89.82, 9.59	0.26, 0.33, 90.97, 8.45
N [He] 2s^2 2p^3	↑↓	↑, ↑, ↑		σ d$_{z^2}$, π d$_{xz}$	2.52, 4.81, 43.09, 49.58	1.78, 3.48, 48.11, 46.62
N_2					16.28, 16.28, 33.72, 33.72	15.16, 16.44, 33.80, 34.60
O [He] 2s^2 2p^4	↑↓	↑, ↑, ↑↓		σ d$_{z^2}$, π d$_{yz}$	0.12, 0.13, 12.30, 87.46	0.12, 0.15, 8.13, 91.60
S [Ne] 3s^2 3p^4	↑↓	↑, ↑, ↑↓		σ d$_{z^2}$, π d$_{yz}$	0.17, 0.17, 22.08, 77.58	0.11, 0.15, 6.10, 93.64

out as very curious cases forming strong bonds enhancing the atomic chains and increasing their lengths, suggesting a possibility to create longer copper NWs synthesized in nitrogen atmospheres.[34] The electronic structure of all impurities bonded to copper LAC atoms was studied showing the differences in bonding for each impurity. DOS and charge densities were presented, and remarks about the possibility of electronic transport in each case was discussed. We hope that the results of the present work can be useful to experimentalists and theorists studying very thin metal NWs.

ACKNOWLEDGMENTS

The simulations were performed at the CENAPAD-SP and IFGW-UNICAMP. We acknowledge support from FAPESP and CNPq. E.P.M.A. was supported by CAPES.

[1] N. Agrait, A. L. Yeyati, and J. M. van Ruitenbeek, Phys. Rep. **377**, 81 (2003) and references therein.
[2] H. Park, J. Park, A. K. L. Lim, E. H. Anderson, A. P. Alivisatos, and P. L. McEuen, Nature (London) **407**, 57 (2000).
[3] S. Diaz-Tendero, S. Folsch, F. E. Olsson, A. G. Borisov, and J. P. Gauyacq, Nano Lett. **8**, 2712 (2008).
[4] S. Diaz-Tendero, F. E. Olsson, A. G. Borisov, and J. P. Gauyacq, Phys. Rev. B **79**, 115438 (2009).
[5] S. Diaz-Tendero, A. G. Borisov, and J. P. Gauyacq, Phys. Rev. Lett. **102**, 166807 (2009).
[6] N. Nilius, T. M. Wallis, and W. Ho, Science **297**, 1853 (2002).
[7] J. Lagoute, C. Nacci, and S. Folsch, Phys. Rev. Lett. **98**, 146804 (2007).
[8] R. B. Pontes, E. Z. da Silva, A. Fazzio, and A. J. R. da Silva, J. Am. Chem. Soc. **130**, 9897 (2008).
[9] V. Rodrigues and D. Ugarte, Phys. Rev. B **63**, 073405 (2001).
[10] F. D. Novaes, A. J. R. da Silva, E. Z. da Silva, and A. Fazzio, Phys. Rev. Lett. **90**, 036101 (2003).
[11] F. D. Novaes, A. J. R. da Silva, A. Fazzio, and E. Z. da Silva, Appl. Phys. A **81**, 1551 (2005).
[12] N. V. Skorodumova and S. I. Simak, Phys. Rev. B **67**, 121404(R) (2003).
[13] N. V. Skorodumova, S. I. Simak, A. E. Kochetov, and B. Johansson, Phys. Rev. B **75**, 235440 (2007).
[14] D. Cakir and O. Gulseren, Phys. Rev. B **84**, 085450 (2011).
[15] F. D. Novaes, A. J. R. da Silva, E. Z. da Silva, and A. Fazzio, Phys. Rev. Lett. **96**, 016104 (2006).
[16] W. H. A. Thijssen, D. Marjenburgh, R. H. Bremmer, and J. M. van Ruitenbeek, Phys. Rev. Lett. **96**, 026806 (2006).
[17] E. P. M. Amorim, A. J. R. da Silva, A. Fazzio, and E. Z. da Silva, Nanotechnology **18**, 145701 (2007).
[18] E. P. M. Amorim and E. Z. da Silva, Phys. Rev. B **81**, 115463 (2010).
[19] O. Gulseren, F. Ercolessi, and E. Tosatti, Phys. Rev. Lett. **80**, 3775 (1998).
[20] E. Tosatti, S. Prestipino, S. Kostlmeier, A. Dal Corso, and F. D. Di Tolla, Science **291**, 288 (2001).
[21] Y. Iguchi, T. Hoshi, and T. Fujiwara, Phys. Rev. Lett. **99**, 125507 (2007).
[22] E. P. M. Amorim and E. Z. da Silva, Phys. Rev. Lett. **101**, 125502 (2008).
[23] Y. Kondo and K. Takayanagi, Science **289**, 606 (2000).
[24] Y. Oshima, A. Onga, and K. Takayanagi, Phys. Rev. Lett. **91**, 205503 (2003).
[25] Y. Oshima, H. Koizumi, K. Mouri, H. Hirayama, K. Takayanagi, and Y. Kondo, Phys. Rev. B **65**, 121401(R) (2002).
[26] J. W. Kang and H. J. Hwang, J. Phys.: Condens. Matter **14**, 2629 (2002).
[27] J. W. Kang, J. J. Seo, and H. J. Hwang, J. Phys.: Condens. Matter **14**, 8997 (2002).
[28] B. Wang, J. Zhao, X. Chen, D. Shi, and G. Wang, Nanotechnology **17**, 3178 (2006).
[29] E. P. M. Amorim, A. J. R. da Silva, and E. Z. da Silva, J. Phys. Chem. C **112**, 15241 (2008).
[30] J. Zhu, D. Shi, J. Zhao, and B. Wang, Nanotechnology **21**, 185703 (2010).
[31] D. Kruger, H. Fuchs, R. Rousseau, D. Marx, and M. Parrinello, Phys. Rev. Lett. **89**, 186402 (2002).
[32] M. Konopka, R. Rousseau, I. Stich, and D. Marx, J. Am. Chem. Soc. **126**, 12103 (2004).
[33] M. Konopka, R. Turansky, M. Dubecky, D. Marx, and I. Stich, J. Phys. Chem. C **113**, 8878 (2009).
[34] E. P. M. Amorim and E. Z. da Silva, Phys. Rev. B **82**, 153403 (2010).
[35] P. Hohenberg and W. Kohn, Phys. Rev. **136**, 864B (1964).
[36] W. Kohn and L. J. Sham, Phys. Rev. **140**, 1133A (1965).
[37] J. M. Soler, E. Artacho, J. D. Gale, A. Garcia, J. Junquera, P. Ordejon, and D. Sanchez-Portal, J. Phys.: Condens. Matter **14**, 2745 (2002).
[38] N. Troullier and J. L. Martins, Phys. Rev. B **43**, 1993 (1991).
[39] S. G. Louie, S. Froyen, and M. L. Cohen, Phys. Rev. B **26**, 1738 (1982).
[40] D. M. Ceperley and B. J. Alder, Phys. Rev. Lett. **45**, 566 (1980).
[41] J. P. Perdew, K. Burke, and M. Ernzerhof, Phys. Rev. Lett. **77**, 3865 (1996).
[42] H. J. Monkhorst and J. D. Pack, Phys. Rev. B **13**, 5188 (1976).
[43] A. Kokalj, Comput. Mater. Sci. **28**, 155 (2003). Code available from http://www.xcrysden.org/.